A CURVE-FITTING TECHNIQUE TO IMPROVE WAVELENGTH CALIBRATIONS OF IMAGING SPECTROMETER DATA

Bo-Cai Gao,[*] Marcos J. Montes,[†] and Curtiss O. Davis[‡]

1 INTRODUCTION

There are now growing interests in hyperspectral remote sensing for research and applications in a variety of fields, including geology, agriculture, forestry, coastal and inland water studies, environment hazards assessment, and urban studies (Mouroulis et al., 2000). The concept of imaging spectrometry, or hyperspectral imaging, was originated from geological communities in the early 1980s (Goetz et al., 1985), mainly for the purpose of mineral exploration. Imaging spectrometers acquire images in many contiguous narrow channels such that for each picture element (pixel) a complete reflectance or emittance spectrum can be derived from the wavelength region covered. Figure 1 shows an example of a spectrum acquired with the Airborne Visible Infrared Imaging Spectrometer (AVIRIS) (Vane et al., 1993; Green et al., 1998) from an ER-2 aircraft at 20 km altitude. The solar radiation on the Sun-surface-sensor path is subject to absorption and scattering by the atmosphere and the surface. Major atmospheric absorption bands, such as those of water vapor centered at approximately 0.94, 1.14, 1.38, and 1.88 μm, the oxygen band at 0.76 μm, the carbon dioxide bands near 2.01 and 2.06 μm, and a solar Fraunhofer line near 0.43 μm are clearly seen. In order to study surface properties using imaging spectrometer data, the atmospheric absorption and scattering effects must be removed. Several atmospheric correction algorithms (e.g., Gao et al., 1993; Gao and Davis; 1997; Adler-Golden et al., 1998; Qu et al., 2000) for deriving surface reflectances from imaging spectrometer data have been developed in the past decade.

For both the airborne and spaceborne imaging spectrometers, shifts in radiometric and spectral calibrations can occur. Calibration coefficients for all detectors obtained in a laboratory may need to be adjusted when applied to

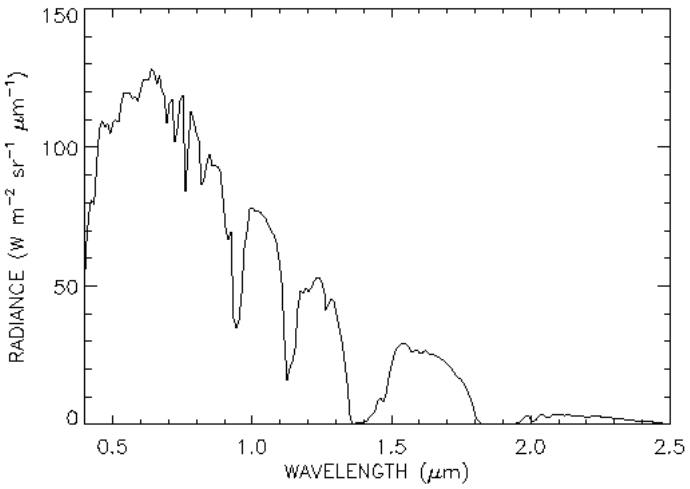

Figure 1: An AVIRIS spectrum showing typical features due to the solar spectrum and gaseous absorption by the terrestrial atmosphere.

[*] Remote Sensing Division, Code 7212, Naval Research Laboratory, Washington, D.C. 20375; Bo-Cai.Gao@NRL.Navy.mil
[†] Remote Sensing Division, Code 7212, Naval Research Laboratory, Washington, D.C. 20375; Marcos.Montes@NRL.Navy.mil
[‡] Remote Sensing Division, Code 7203, Naval Research Laboratory, Washington, D.C. 20375; Curtiss.Davis@NRL.Navy.mil

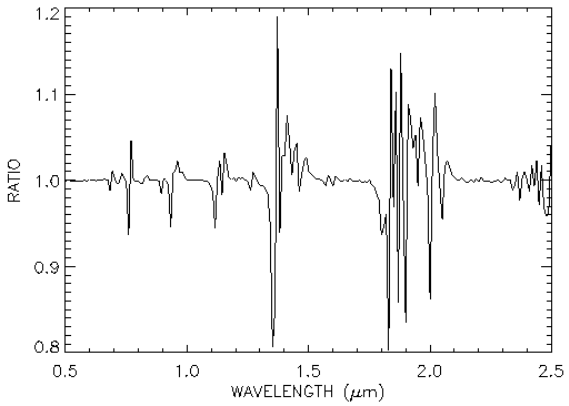

Figure 2: The ratio of two simulated transmission spectra with a spectral resolution of about 10 nm but with a relative wavelength shift of 1 nm between them. Over regions where there are absorption bands of atmospheric gases, the ratio values deviate significantly from 1.0.

data obtained from an aircraft or a satellite platform. Shifts in channel center wavelengths and changes in spectral resolution may occur when an instrument is airborne or spaceborne due to vibrations, and to changes in instrument temperature and pressure. In order to use radiative transfer-based approach to derive surface reflectances from hyperspectral imaging data for improved studies of surface properties, accurate radiometric and spectral calibration to the data must be made (Green, 1998).

Following calibrations, atmospheric correction algorithms are typically applied to imaging spectrometer data to remove the effects of atmospheric gas absorption, and Rayleigh and aerosol scattering (Gao et al., 1993). The atmospheric gas absorption features are very sharp and errors in wavelength calibrations can produce significant errors in the retrieved land or ocean surface reflectances around these features. For the purpose of illustrating the importance of wavelength calibrations, we calculated two spectra at the typical AVIRIS resolution of approximately 10 nm. One spectrum was calculated for the correct wavelengths, and the other with a 1 nm shift in wavelengths for all the channels. Figure 2 shows the ratio of the two spectra. Over regions where there are absorption bands of atmospheric gases, the ratio values deviate significantly from 1. Therefore, small errors in wavelength positions can introduce large errors in the derived reflectance spectra.

In this paper, we describe an algorithm for refining spectral calibrations of imaging spectrometer data. The algorithm is based on spectrum-matching of atmospheric water vapor, oxygen, and carbon dioxide bands, and solar Fraunhofer lines. We then present sample results from applications of the algorithm to data acquired with a few airborne and spaceborne hyperspectral imaging sensors.

2 METHOD

Spectrum-matching techniques (Chang and Shaw, 1977) were developed in the 1970s for retrieving positions and widths of atmospheric gases from laboratory-measured "ultra" spectra (in which individual lines within bands of atmospheric gases are resolved). Later on, a spectrum-matching technique was developed for deriving column atmospheric water vapor amounts (Gao and Goetz, 1990) from hyperspectral imaging data (in which major bands of atmospheric gases are resolved) acquired with the AVIRIS instrument. We have recently developed another spectrum-matching algorithm for refining wavelength calibrations of imaging spectrometer data. This algorithm is based on the matching between measured atmospheric water vapor, oxygen, carbon dioxide bands, and solar Fraunhofer lines with the corresponding calculated bands. The spectral calculations are performed using procedures described by Gao et al. (2000) and Gao and Davis (1997), which utilize high-resolution line-by-line atmosphere transmittance calculations based on the HITRAN 2000 database.[§]

In order to automate the wavelength calibrations of hyperspectral data based on atmospheric or solar Fraunhofer band matching, we assume that the wavelengths of the measured spectrum can shift from –5 nm to +5

[§] Rothman et al., 2001 private communication.

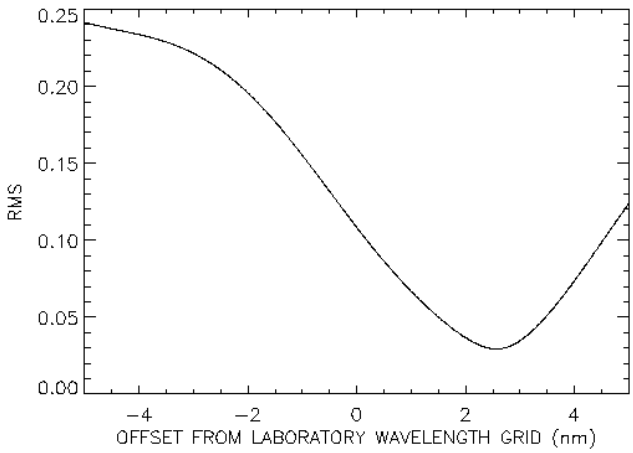

Figure 3: Standard deviation between the laboratory calibration spectra and the modeled spectra as a function of wavelength shift.

nm in steps of 0.01 nm. For each step, we calculate the standard deviation between the measured and the simulated spectrum. Figure 3 shows the standard deviation of matching for a PHILLS (Portable Hyperspecral Imager for Low Light Spectroscopy) spectrum in the vicinity of the 0.76 μm oxygen feature as a function of wavelength shift. A minimum occurs at a wavelength shift of 2.57 nm, so this is considered to be our best estimate of the wavelength shift.

In the case of hyperspectral images measured with sensors built with arrays of area detectors, each across track pixel may have a different wavelength calibration. The spectrum-matching technique described above needs to be applied to each cross track pixel of the data. In our practical applications, we average (in the along track direction) all the spectra of a scene for a particular cross track sample to improve signal-to-noise ratio, and apply the spectrum-matching technique to the averaged spectrum to obtain an estimate of wavelength shift for the column. The process is repeated for every cross track pixel in the imaging scene.

Through theoretical considerations and analysis of measured imaging spectrometer data, we have found that a number of atmospheric and solar bands in the 0.4 – 2.5 μm solar spectral region can be useful for wavelength calibrations using the spectrum-matching technique described above. Specifically, for instruments with a spectral resolution of approximately 10 nm, the atmospheric water vapor bands centered near 0.82, 0.94, 1.14 μm, the oxygen band near 0.76 μm, and the carbon dioxide bands near 1.58 and 2.06 μm can be used for wavelength calibrations. For instruments with a spectral resolution of about 5 nm, an additional solar Fraunhofer line near 0.43 μm becomes useful due to the increased resolving power of the instruments. For instruments having a spectral resolution of 2.5 nm or better, several more solar Fraunhofer lines centered near 0.516, 0.656, 0.854, and 0.863 μm, can be used for wavelength calibrations because of the further increased resolving powers.

3 RESULTS

Our spectrum-matching algorithm has been applied to hyperspectral data collected with several imaging spectrometers for refining wavelength calibrations. Sample results from applications to AVIRIS, PHILLS, and Hyperion data are described below.

3.1 *AVIRIS*

We typically average all the 512 spectra in one along track column of a scene to obtain a spectrum with signal to noise ratios well above 1000 before applying our spectrum-matching technique to AVIRIS data. The spectrum-matching technique is then applied to the averaged spectrum to estimate wavelength shift from the supplied laboratory AVIRIS calibrations. Sample wavelength shifts obtained from an AVIRIS data set are shown in Figure 4. The AVIRIS data used in this study was acquired over the Cuprite (30^o 30'N and 117^o 10' W) mining district in Nevada on 23 June 1995. The three curves in Fig. 4 are wavelength shifts as a function of sample number (cross track direction). These wavelength shifts are obtained through matching an atmospheric oxygen band near

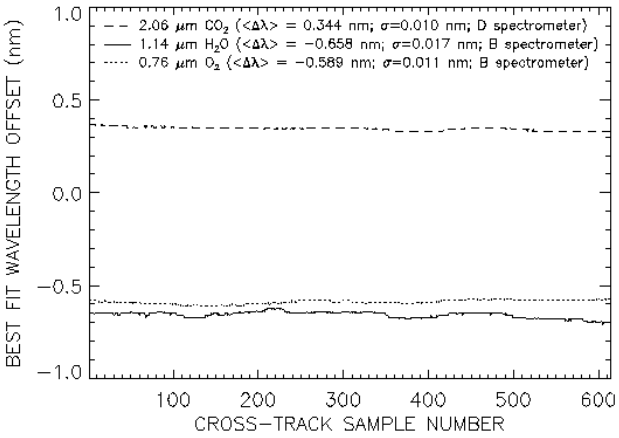

Figure 4. AVIRIS wavelength offsets derived through spectrum-matching of an oxygen band near 0.76 μm, a water vapor band near 1.14 μm, and a carbon dioxide band near 2.06 μm.

0.76 μm, a water vapor band near 1.14 μm, and a carbon dioxide band near 2.06 μm. Both the oxygen and the water vapor bands are located in the wavelength region covered by the Spectrometer B of AVIRIS. The carbon dioxide band is located in the wavelength range covered by the Spectrometer D. The mean of wavelength shifts from fitting the oxygen band for all the samples is –0.589 nm with a standard deviation of 0.011 nm. This mean shift is within the AVIRIS' laboratory wavelength calibration uncertainty of ±1 nm. Because AVIRIS is a scanning instrument, the shift is essentially the same across the scene. The mean shift can be considered to be the best estimate of AVIRIS' wavelength shift based on the oxygen-band-fitting. The standard deviation of 0.012 nm can be considered to be the accuracy using the spectrum-matching technique for wavelength calibrations. The mean wavelength shift obtained from fitting the 1.14-micron water vapor band is –0.658 nm with a standard deviation of 0.017 nm. This mean shift is consistent with the mean shift obtained from fitting the oxygen band. The mean shift derived from fitting the CO_2 band near 2.06 μm is +0.344 nm with a standard deviation of 0.010 nm. The wavelength shift for the Spectrometer D is positive while that for the Spectrometer B is negative. The amounts of shifts are all within the stated AVIRIS' laboratory calibration accuracy of ±1 nm.

3.2 *PHILLS*

Over the past few years the Naval Research Laboratory (NRL) has build a series of PHILLS instruments (Davis, et al., 1999; Davis et al., 2002). All the PHILLS instruments use area arrays in focal planes. The PHILLS instruments have spectral resolution of 1.13 nm per pixel and are typically binned by 4 to 4.52 nm. Data collections

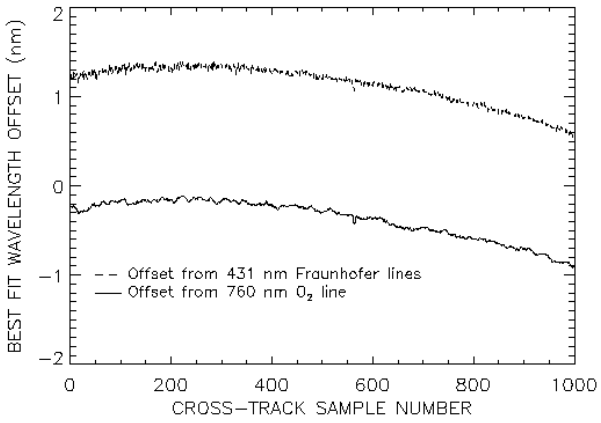

Figure 5: PHILLS wavelength offsets based on fitting an oxygen band near 0.76 μm and a solar band at 0.431 μm.

have been made from low altitude airplane platforms during several field experiments. The temperature and pressure around the PHILLS instruments have not been controlled during the data acquisitions. Our spectrum-matching technique has been applied to the column-averaged PHILLS spectra for estimating wavelength offsets. Sample results obtained from one PHILLS data set are shown in Figure 5. The PHILLS data with a spectral resolution of 4.52 nm were acquired over an area in New Jersey (39°20' N and 74°30' W) on 31 July 2001. The two curves in Fig. 5 are wavelength offsets (as a function of sample number in the cross track direction) derived through matching the oxygen band near 0.76 μm and a solar Fraunhofer line near 0.43 μm. The offset curve from the oxygen band matching shows a difference of about 0.7 nm from left side of the detector array to the right side of the array. This is the result of a combination of spectral smile of about 0.3 nm over 1000 pixels and a tilt of about 0.6 nm over 1000 pixels caused by misalignment between the spectrometer and the camera. The two curves in Fig. 5 have a vertical offset of approximately 1.3 nm, indicating a possible change in light dispersion property for the PHILLS instrument in the aircraft environment.

3.3 *Hyperion*

TRW Space, Defense and Information Systems in Los Angeles, CA built the Hyperion instrument. It is the first spaceborne imaging spectrometer flying on a NASA experimental satellite platform named Earth Observer-1 (EO-1) (Ungar, 1997). This instrument was launched into space in November 2000. It covers the 0.4 – 2.5 μm reflected solar spectral region with more than 220 narrow channels at a spectral sampling spacing of about 10 nm. It has a spatial resolution of 30 m on the ground, and a surface swath width of 7 km (Ungar, 1997). The dashed line in Figure 6 is the curve of center wavelength position for Band 41 as a function of sample number in the satellite cross track direction. The center wavelengths were obtained based on laboratory calibrations of the Hyperion sensor at TRW. Because the center wavelengths depend on the sample number, the "smile" effect is obviously present in the Hyperion sensor. The dotted line in Fig. 6 is a curve of our estimated center wavelength positions based on matching the 0.76 μm oxygen band from one set of Hyperion data acquired over the Cuprite mining district in Nevada on March 1, 2001. This curve is shifted upward by roughly 1 nm in comparison with the laboratory calibration curve. Actually, the amount of shifts depends slightly on the sample number. The solid line in Fig. 6 is our estimates of center wavelengths for Band 41 from another Hyperion data set acquired over the heavily vegetated Coleambally Irrigation Area (39°48' S, 145°39' E) in Australia on March 6, 2001. The shape of this curve is very similar to that of the Cuprite curve. The similarity of the two curves (one from a heavily vegetated area, one from a much less vegetated area) provides evidence that we are correctly accounting for the differing backgrounds in the vicinity of the 0.76 μm feature.

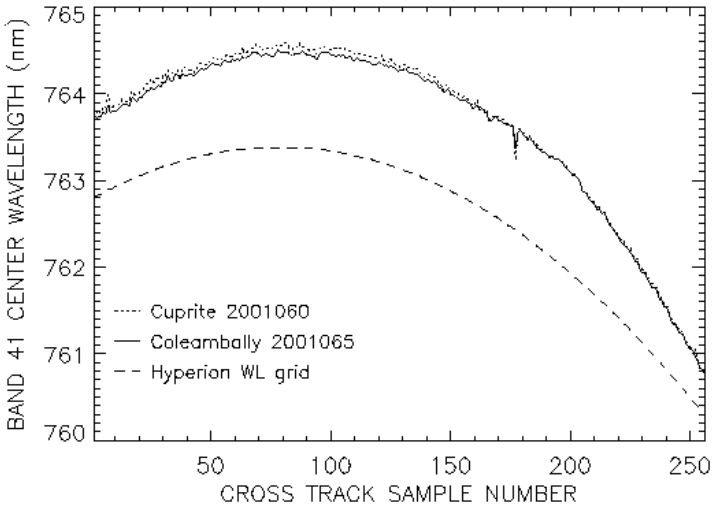

Figure 6: Center wavelengths as a function of sample number in the cross track direction for Channel 41 of the Hyperion instrument obtained from laboratory calibration (dashed line) and retrieved from the Cuprite Hyperion data set (dotted line) and from the Coleambally Hyperion data set (solid line) based on spectrum-matching of the oxygen band near 0.76 μm.

4 DISCUSSIONS

The application of our algorithm to AVIRIS data has demonstrated that the channel positions can be estimated with an accuracy of 0.017 nm or better using our spectrum-matching technique, while the AVIRIS' laboratory calibration uncertainty is about ± 1 nm. Therefore, improved wavelength calibrations can be obtained using the spectrum-matching technique. After adjusting the standard AVIRIS wavelength table based on our results, errors in derived surface reflectance spectra using atmospheric correction algorithms will be decreased significantly, particularly over spectral regions where the atmospheric gas absorption features are strong.

For array spectrometers, the spectral calibration may vary across the scene as a result of spectral smile or misalignment. The applications of our spectrum-matching algorithm to the PHILLS data and Hyperion data have shown that our algorithm is sufficiently accurate to allow the measure of these artifacts. Corrections of these artifacts, in particular the misalignment, are possible for airborne imaging spectrometers.

5 SUMMARY

We have developed a spectrum-matching algorithm for refining the wavelength calibrations of imaging spectrometer data. Atmospheric water vapor, carbon dioxide, oxygen bands, and solar Fraunhofer lines are used for the spectrum matching. The algorithm has been applied to data acquired with the AVIRIS, PHILLS, and Hyperion instruments onboard aircraft or satellite platforms. After the refinement in wavelength calibrations, improved derivation of surface reflectance spectra from hyperspectral imaging data based on radiative transfer modeling can be obtained. Subsequently, better studies of surface properties using the derived surface reflectance spectra can be conducted.

6 ACKNOWLEDGEMENTS

The authors gratefully acknowledge the support of the U.S. Office of Naval Research for this research.

7 REFERENCES

Adler-Golden, S., A. Berk, L. S. Bernstein, S. Richtsmeier, P. K. Acharya, M. W. Matthew, G. P. Anderson, C. L. Allred, L. S. Jeong, and J. H. Chetwynd, 1998, "FLAASH, A MODTRAN4 atmospheric correction package for hyperspectral data retrievals and simulations", *in Proceedings of the Seventh JPL Airborne Earth Science Workshop, Jan. 12 - 16 (Editor: R. O. Green)*, JPL Publication 98-21, 1, 9-14, Jet Propul. Lab., Pasadena, CA.

Chang, Y. S., and J. H. Shaw, 1977, "A nonlinear least squares method of determining line intensities and half-widths", Appl. Spectroscopy, 31, 213-220.

Davis, C. O., M. Kappus, J. Bowles, J. Fisher, J. Antoniades, and M. Carney, 1999, "Calibration, characterization and first results with the ocean PHILLS hyperspectral imager", SPIE, 3753, 160-167.

Davis, C. O., J. Bowles, R. A. Leathers, D. Korwan, T. V. Downes, W. A. Snyder, W. J. Rhea, W. Chen, J. Fisher, W. P. Bissett, and R. A. Reisse, 2002, "Ocean PHILLS hyperspectral imager: design, characterization, and calibration", *Optics Express*, 10, 210-221.

Gao, B.-C., and A. F. H. Goetz, 1990, "Column atmospheric water vapor and vegetation liquid water retrievals from airborne imaging spectrometer data", *J. Geophys. Res.*, *95*, 3549-3564.

Gao, B.-C., K. H. Heidebrecht, and A. F. H. Goetz, 1993, "Derivation of scaled surface reflectances from AVIRIS data," *Remote Sens. Env.*, 44, 165-178.

Gao, B.-C., and C. O. Davis, 1997, "Development of a line-by-line-based atmosphere removal algorithm for airborne and spaceborne imaging spectrometers", in *SPIE Proceedings, Vol. 3118*, 132-141.

Gao, B.-C., M. J. Montes, Z. Ahmad, and C. O. Davis, 2000, "Atmospheric correction algorithm for hyperspectral remote sensing of ocean color from space", Appl. Opt., 39, 887-896.

Goetz, A. F. H., G. Vane, J. Solomon, and B. N. Rock, 1985, "Imaging spectrometry for earth remote sensing," *Science, 228*, 1147-1153.

Green, R. O., M. L. Eastwood, C. M. Sarture, T. G. Chrien, M. Aronsson, B. J. Chippendale, J. A. Faust, B. E. Parvi, C. J. Chovit, M. Solis, M. R. Olah, and O. Williams, 1998, "Imaging spectrometry and the Airborne Visible/Infrared Imaging Spectrometer (AVIRIS)", Remote Sens. Env., 65, 227-248.

Green, R. O. , 1998, "Spectral calibration requirement for Earth-looking imaging spectrometers in the solar-reflected spectrum", Appl. Opt., 683-690.

Mouroulis, P., R. O. Green, and T. G. Chrien, 2000, "Design of pushbroom imaging spectrometers for optimum recovery of spectroscopic and spatial information", Appl. Opt., 39, 2210-2220.

Qu, Z., A. F. H. Goetz, and K. B. Heidebrecht, 2000, "High accuracy atmospheric correction for hyperspectral data (HATCH)", in Proceedings of the *Ninth JPL Airborne Earth Science Workshop, Feb. 23 - 25 (Editor: R. O. Green)*, JPL Publication 00-18, 1, 373-380, Jet Propul. Lab., Pasadena, CA.

Ungar, S. G. , 1997, "Technologies for future Landsat missions", Photogarm. Eng. & Remote Sens., 63, 901-905.

Vane, G., R. O. Green, T. G. Chrien, H. T. Enmark, E. G. Hansen, and W. M. Porter, 1993, "The Airborne Visible/Infrared Imaging Spectrometer," *Remote Sens. Env.*, *44*, 127-143.